

Visual and Inertial Datasets for an eVTOL Aircraft Approach and Landing Scenario

Nelson Brown¹

NASA Armstrong Flight Research Center, Edwards, California, 93523, USA

Evan Kawamura²,

NASA Ames Research Center, Moffett Field, California, 94035, USA

Luke Bard³, A. J. Jaffe⁴, Wayne Ringelberg⁵,

NASA Armstrong Flight Research Center, Edwards, California, 93523, USA

Keerthana Kannan⁶, and Corey Ippolito⁷

NASA Ames Research Center, Moffett Field, California, 94035, USA

A National Aeronautics and Space Administration (NASA) project developing computer vision algorithms for autonomous flight is producing real-world datasets with cameras mounted on aircraft. In related domains, such as autonomous driving, open datasets are key to innovation and advancement in computer vision and autonomous perception for future Advanced Air Mobility (AAM) operations. Few vision datasets, however, are publicly available in the aviation context. This paper introduces preliminary datasets containing several examples of approach and landing scenarios. The platform aircraft include a multirotor small unmanned aerial system (sUAS) and a crewed helicopter as surrogates for future electric vertical take-off and landing (eVTOL) aircraft. The dataset provides video imagery with associated inertial navigation system-global positioning system (INS-GPS) position and attitude estimates and other sensors. Surveyed locations of the visual features of the landing area are included. This dataset is the first to be released in an ongoing effort to collect and share large, diverse datasets relevant to autonomous aviation; community critique that can inform and improve future flight campaigns is welcome.

I. Introduction

The National Aeronautics and Space Administration (NASA) Transformational Tools and Technologies (TTT) project is developing technologies to support Advanced Air Mobility (AAM). Some of those technologies include computer vision systems for autonomous flight in urban areas, as depicted in Fig 1.

¹ Aerospace Engineer, Controls & Dynamics Branch, non-member.

² Computer/GNC Engineer, Intelligent Systems Division, AIAA member.

³ Meteorologist, Aerodynamics & Propulsion Branch, non-member.

⁴ Lead Operations Engineer, Operations Engineering Branch, non-member.

⁵ Research Test Pilot, Flight Crew Branch, non-member.

⁶ Embedded Software Developer, Intelligent Systems Division, AIAA member.

⁷ Aerospace Scientist, Intelligent Systems Division, AIAA member.



Fig. 1 An artist's concept image of an AAM aircraft approaching to land on a rooftop helipad. (Depiction courtesy NASA Graphics.)

Computer vision development relies heavily on datasets collected in an application-relevant context, with reliable ground-truth data for evaluation. In the domain of autonomous driving, many datasets have been collected and published by various research teams around the world. Two well-known examples are the KITTI datasets (<https://www.cvlibs.net/datasets/kitti/>) produced by Karlsruhe Institute of Technology and Toyota Technological Institute at Chicago [1] and the Waymo Open Dataset (<https://waymo.com/open/>) produced by Waymo LLC [2].

Some datasets have been released in the context of small unmanned aerial system (sUAS) operations at very low altitudes, such as VIRAL [3]. The EuRoC Micro Aerial Vehicle Datasets [4], recorded indoors, are commonly used to evaluate SLAM algorithms such as ORB-SLAM3 and OV²SLAM [5,6].

We have yet, however, to see datasets utilized in training and evaluating autonomous perception in the context of AAM passenger aviation. The TTT project thus has set out to produce datasets needed for its own computer vision research needs, especially video representative of the perspective of a notional AAM vehicle coupled with ground-truth trajectory data.

The TTT project is developing a sensor payload for aircraft with plans to collect large datasets in a variety of diverse flight situations. In preparation for this larger data collection campaign, the project team conducted several preliminary flights with an sUAS and a helicopter. We are sharing these preliminary datasets with the broader community to help foster development of autonomy and perception in the aviation domain. The NASA plans are to continue adding to these open collections; the community is invited to provide feedback through the website <https://nari.arc.nasa.gov/ttt-ram/data> toward improving the quality and relevance of the corpus.

II. Flight Scenarios

The preliminary flight campaigns were focused on collecting video of approach and landing scenarios to support research activities in computer-vision based precision positioning and navigation. The landing scenario represents a notional future passenger electric vertical take-off and landing (eVTOL) aircraft approach and landing at a helipad, as envisioned in Fig. 1. The datasets collected during these campaigns supported the work presented in Refs [7-9]. Sample images from the recorded approaches are shown in Fig. 2.



Fig 2. Sample images from several landing approach segments.

The images in each row are taken from the beginning, middle, and end of an approach segment of videos from different scenarios. Some segments captured ground vehicles or birds crossing in front of the aircraft, and the imagery includes ground obstacles such as towers, light poles, and trees. In the first row of Fig. 2 are examples from the sUAS approach to the NASA Armstrong Flight Research Center (AFRC) (Edwards, California) 01H helipad. The second- and third-row images are examples of nighttime and daytime helicopter approaches to the NASA Kennedy Space Center (KSC) Operational Health Facility (OHF) helipad (Kennedy Space Center, Florida). The fourth-row images are examples of a helicopter approach to elevated platform in a low-density urban environment (Melbourne, Florida).

While the test platforms are an sUAS (Fig. 3(a)) and a helicopter (Fig. 3(b)), the trajectory chosen for these flight campaigns is modeled on 6- and 9-degree glideslope approach and landing trajectories for a notional passenger eVTOL, borrowed from the NASA Advanced Air Mobility (AAM) project [10].



Fig. 3(a) The sUAS data collection platform: Freely Alta 8 sUAS with a RED DSMC2 camera mounted on a Movi Pro gimbal. (Photograph courtesy Nelson Brown, AFRC.)



Fig. 3(b) The helicopter data collection platform: Airbus H135 with WESCAM MX-10. (NASA photograph number KSC-20201027-PH-KLS01_0040.)

The platform sUAS aircraft initiated each approach from approximately 1500 ft (460 m) downrange at an altitude of 250 ft (76 m) above ground level (AGL). An example of the sUAS trajectory is illustrated in Fig. 4.



Fig. 4 Example segment of the sUAS approach trajectory landing at the NASA Armstrong Flight Research Center 01H helipad starting at an altitude of 250 ft (76 m) and 1500 ft (460 m) downrange.

The helicopter initiated most approaches from 2.0 nm (3700 m) downrange and an altitude of 2000 ft (600 m) AGL. Other helicopter approaches initiated from 1500 ft (500 m) AGL for a shallower glideslope to the landing area. The helicopter segments include approaches to the groundlevel helipad at the OHF at KSC, visualized in Fig. 5, and at an elevated platform helipad on the roof of a hospital. The helicopter segments include various lighting conditions at dawn, midday, dusk, and night.

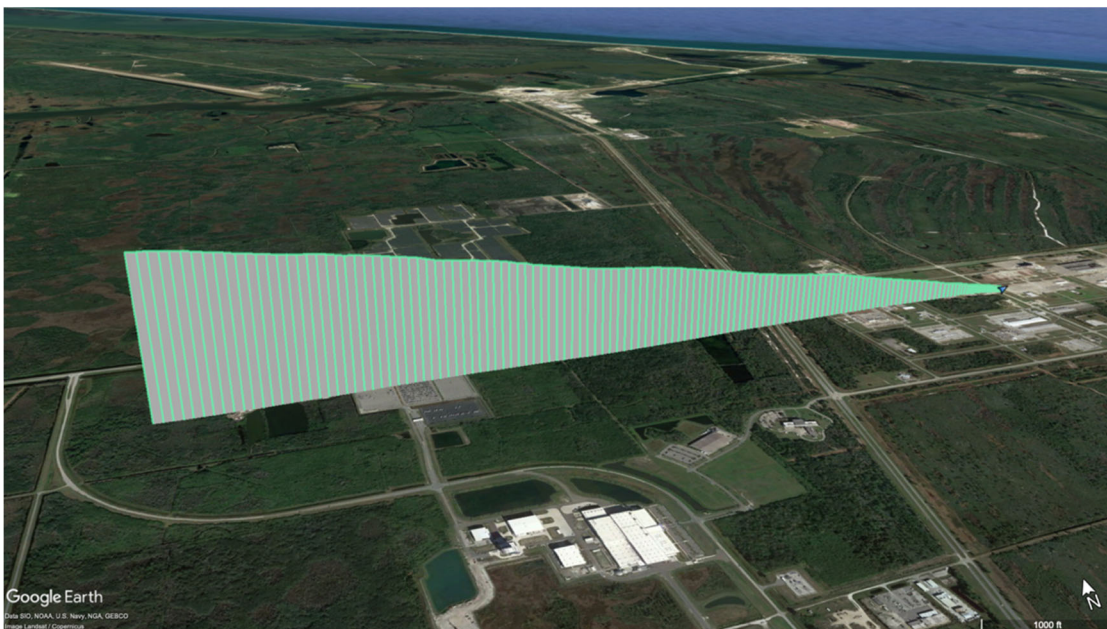


Fig. 5 Example segment of the helicopter approach trajectory to the NASA Kennedy Space Center Operational Health Facility helipad starting from an altitude of 2000 ft (600 m) AGL and 2.0 nm (3700 m) downrange.

The sUAS pilots used waypoint guidance to set up at the initial point of the approach and then switched to manual control to follow the approach trajectory. Starting each approach, the pilots used first-person view (FPV) by way of telemetered video. At approximately 250 ft (76 m) from the touchdown and liftoff area (TLOF), the pilots switched to watching the aircraft directly. During the approach, the ground control officer called out the altitude and if the aircraft was high or low relative to the intended glideslope.

The dataset consists of several repeats of the approach on a heading of 238 deg to the NASA 01H helipad (34°57'32.73"N, 117°52'54.25"W). The overhead view of the landing area in Fig. 6 was captured by the sUAS camera at an altitude of 500 ft (150 m) above the surface.



Fig. 6 Overhead view of the 01H helipad taken by the sUAS at the Armstrong Flight Research Center roughly aligned with north at the top of the image.

The OHF helipad at KSC is located at 28°31'20.5"N, 80°39'10.7"W. Fig. 7 shows the Google Earth imagery from January 2022.



Fig. 7 Google Earth overhead view of the Operational Health Facility helipad at the Kennedy Space Center.

A mobile Pulse Light Approach Slope Indicator (PLASI) is visible in most of the sUAS approach videos. The purpose of a PLASI is to help a pilot execute a stabilized approach to a runway or helipad. During the sUAS flights, however, our remote pilots could not consistently see the PLASI in video downlink and so elected not to rely on it. In a subset of the approach runs, traffic cones were placed around the TLOF. The PLASI and traffic cones are pictured in Fig. 6 and Fig. 8 and are present in the top row of images in Fig. 2. Geographic locations for the PLASI and traffic cones are available in the datasets.

All the segments in this initial dataset were recorded in day or night visual meteorological conditions (VMC). In some cases, there were winds and gusts that caused the aircraft to move.



Fig. 8 Photograph taken facing southwest of the TLOF marked with traffic cones and adjacent PLASI (right). (Photograph courtesy Nelson Brown, AFRC.)

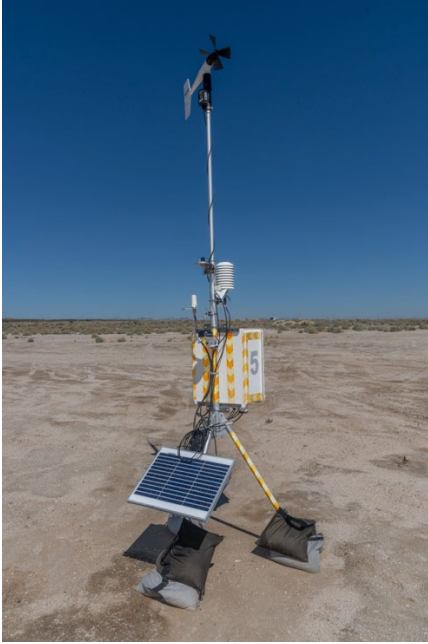
III. The sUAS Vehicle and Sensors

The platform sUAS used for this flight campaign is the FreeFly Alta 8 (Freefly Systems, Woodinville, Washington). The camera is a RED DSMC2 (RED Digital Cinema, LLC, Foothill Ranch, California) mounted on a Movi Pro gimbal (Freefly Systems, Woodinville, Washington). This configuration is a typical one for this sUAS and is frequently used in the movie and video production industry.

The production flight controller for the Alta 8 sUAS is a Pixhawk 2.1 Blue Cube (CubePilot Pty. Ltd., Victoria, Australia). Flight data logs from the Pixhawk are included in the dataset in the native “ulog” format, as well as files converted with the pyulog utility (<https://github.com/PX4/pyulog>) in Keyhole Markup Language (KML) and comma-separated values (CSV) text files for convenience.

The Movi Pro gimbal also logs data in CSV format, and includes the time histories of gimbal joint positions, which are helpful for understanding the orientation of the camera relative to the Pixhawk flight controller to compare vision-algorithm-derived trajectories to the INS-GPS estimated trajectory.

Nearby weather stations, seen in Fig. 9, recorded surface meteorological conditions near the helipad.



a



b

Fig. 9(a): Campbell Scientific Inc. weather station measuring wind speed and direction, temperature, humidity, station pressure, solar insolation, and calculated density altitude. (NASA photograph number AFRC2023-0139-11); and, (b): Radiometrics model 4000 mini SODAR for measuring wind velocities. (NASA photograph number AFRC2023-0139-20.)

These stations (Campbell Scientific Inc., Logan, Utah), one of which is shown in Fig. 9a, recorded 1-min average measurements of wind speed and direction, temperature, humidity, station pressure, solar insolation, and calculated density altitude. The weather stations produced ASCII text files than can be easily converted to CSV format. Surface measurements were augmented by a Sound Detection and Ranging (SODAR) system monitoring three-dimensional wind profiles in the planetary boundary layer. The SODAR system (Radiometrics model 4000 mini SODAR), shown in Fig. 9b, recorded two-minute average wind velocities 20m to 250m AGL above the unit every 5m. The SODAR system outputs data files in CSV format.

IV. The Helicopter Vehicle and Sensors

The platform helicopter used for this flight campaign is the Airbus H135 (Airbus, Toulouse, France). The camera is a WESCAM MX-10 (L3HarrisTechnologies, Inc., Melbourne, Florida). This configuration is a common one for this helicopter and is frequently used by law enforcement and for search and rescue. This camera recorded HD 1080P (1920 x 1080) resolution at 30 frames per second.

The avionics for the Airbus H135 helicopter are developed by Airbus and marketed as Helionix. Flight data logs in A717 format were converted using the National Transportation Safety Board Crash Investigation & Data Event Recovery (CIDER) software.

The WESCAM MX-10 camera records a data overlay in the video imagery, as seen in Fig. 11. The team used optical character recognition (OCR) to extract numerical values from the imagery. These values include the time histories of gimbal pan and tilt angles, which are helpful for understanding the orientation of the camera relative to the helicopter to compare vision-algorithm-derived trajectories to the INS-GPS estimated trajectory. A second video stream without the overlay is recorded concurrently. Video files without the overlay are labeled “clean” in the dataset.

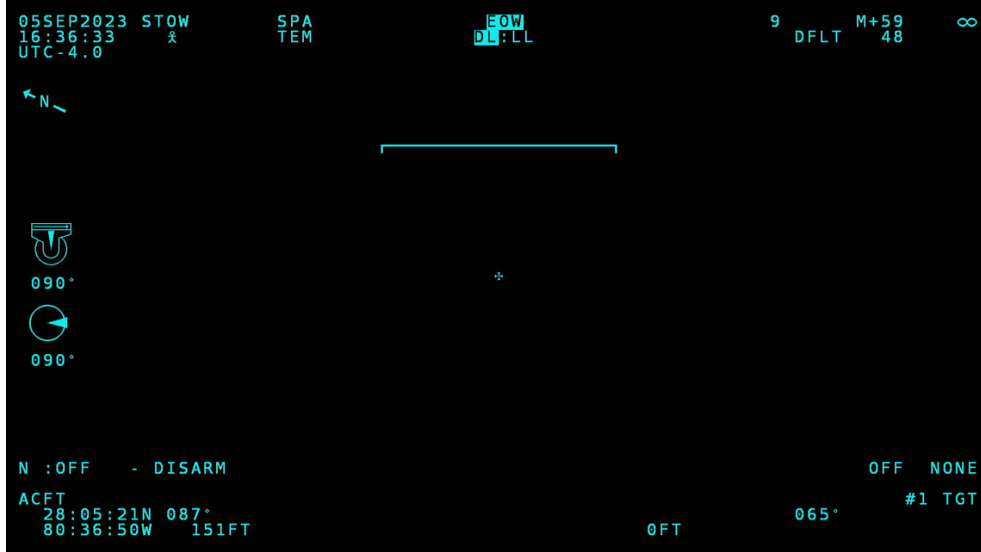


Fig. 11 The video data overlay provided by the WESCAM MX-10 camera includes the pan and tilt angles of the camera gimbal on the left edge of the image.

Nearby weather stations and wind profilers recorded meteorological conditions. On the KSC range, there are various meteorological towers that collect in-situ measurements of wind, pressure, temperature, and humidity at several heights above the ground, from 6 to 492 ft AGL depending on the tower. There are two wind profilers, 48 MHz and 915 MHz, that remotely measure horizontal wind speed and direction from 1,869 to 19,505 m AGL every 150 m, and from 100 to 5,100 m AGL every 100 m, respectively. Weather data from KSC was accessed from their online database (<https://kscweather.ksc.nasa.gov>). Standard hourly surface weather conditions were recorded by the automated surface observation system (ASOS) located at the Melbourne Orlando International Airport (ICAO: KMLB), accessed through the Iowa State Mesonet online database (<https://mesonet.agron.iastate.edu>).

V. Time Synchronization

Several of the data recorders used in these flights log timestamps from the global positioning system (GPS), including the Pixhawk flight controller, the Movi Pro gimbal, the SODAR system, and the weather stations. Our attempts to inject time into the camera electronically were unsuccessful, so the video alignment with time is estimated either from holding a smartphone displaying GPS time in view of the sUAS camera prior to takeoff, or from an event that is easily identified in the Pixhawk flight controller logs such as takeoff or landing.

The helicopter video overlay includes the local time, which is based on GPS time. The overlay time is captured by the OCR process, and linear regression is used to estimate a time vector associated with the video frame index number. Errors in the time offset and drift across the duration have not been quantified.

VI. Camera Intrinsic

To support automatic calibration tools, the team imaged test patterns, including grids of AprilTag visual fiducials (<https://april.eecs.umich.edu/software/apriltag>), printed and mounted on rigid posterboard. The raw calibration images, like the examples in Fig. 12, are included alongside the video for users of the dataset to apply their own calibration methods. The examples show the AprilTag grids intended to be used with the MATLAB Computer Vision Toolbox™ (The MathWorks, Inc., Natick, Massachusetts) calibration procedure (<https://www.mathworks.com/help/vision/ug/camera-calibration-using-apriltag-markers.html>). The team has also imaged circle grids, checkerboards, and an alternative AprilTag grid pattern generated by Kalibr scripts (<https://github.com/ethz-asl/kalibr/wiki/calibration-targets>).

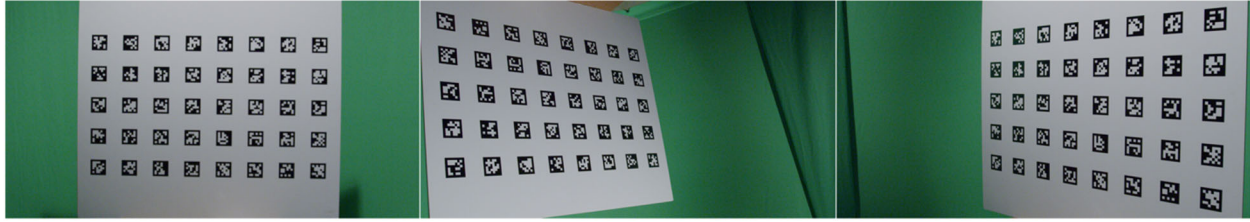


Fig. 12 Examples of calibration images from the RED DSMC2 camera.

The camera mounted on the sUAS uses the HELIUM 8K S35 (RED Digital Cinema, LLC, Foothill Ranch, California) sensor and a Canon EF 16-35mm f/2.8L II lens (Canon, Tokyo, Japan) set to its widest-angle zoom, focal length 16 mm.

The camera mounted on the helicopter has an integrated zoom lens which was set to its widest-angle zoom, focal length 8mm. Presently the datasets available were all recorded in the electro-optical (EO) mode.

The focal distance was manually controlled to be near infinity during flight and during filming of the calibration boards.

VII. Camera Extrinsic

Both cameras used for these datasets are mounted to their platform aircraft on a gimbal. Both gimbals have joints for pan and tilt angles; the sUAS gimbal also has a roll joint. The gimbal joint angle time histories are included in the datasets, and these gimbal joint angles relate the camera attitude to the aircraft body attitude recorded from the aircraft navigation sensors. The linear offset from the camera principal point to the gimbal joint axes and the aircraft center of navigation have not yet been measured. If these offsets become relevant to one or more users of the datasets, they will be measured and added to the online documentation that accompanies the data.

VIII. Dataset Formats and Access

The sUAS camera recorded video in the REDCODE RAW format used by the Red DSMC2 camera in R3D files (<https://www.red.com/red-tech/redcode-raw>). The team uses the REDCINE-X Pro software provided by the camera manufacturer to export the imagery to more common image and video formats.

The helicopter video was recorded in Apple (Apple, Cupertino, California) ProRes codecs in MOV files and converted to more common formats using the ffmpeg utility (<https://www.ffmpeg.org>).

The conversion process requires choices regarding color, contrast, resolution, and compression. The team requests community feedback regarding alternative choices that may improve the performance of computer vision algorithms.

Raw data from the meteorological ground stations are stored in CSV text files. Documentation describing the meteorological parameters are available for download alongside the datasets.

Selected segments of imagery and data are hosted online for the research community to access. The sensor time history data are provided in HDF5 and ros2bag formats. The converted imagery is provided in MOV, JPEG, and PNG.

The team has chosen to parcel out the datasets into archive files not larger than 5 GB to encourage downloads by researchers in the community. In most cases the team needed to reduce the video data by some combination of reducing resolution, reducing frame rate, or applying lossy compression. The team will consider hosting larger, higher-fidelity alternatives in response to community feedback through the project website. Links to these datasets can be found at <https://nari.arc.nasa.gov/ttt-ram/data>.

IX. Future Work

The TTT project is presently developing a sensor package, shown in Fig. 13, to be carried by host aircraft such as the NASA helicopters. The new sensor pod would include additional cameras and sensors and increase the precision of the calibration and time-correlation between the sensors. Lessons learned from the flight campaigns for the datasets described in this paper, combined with feedback from computer vision researchers within NASA and in the broader research community, are guiding the requirements development for the sensor pod and future flight campaigns.

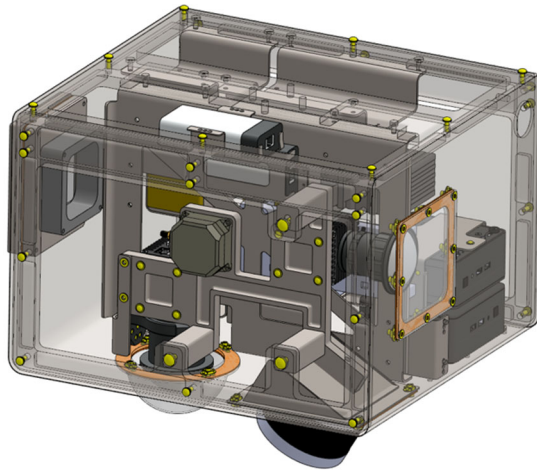


Fig. 13 The preliminary design of a sensor package for future data collection.

The new sensor pod would be rigidly attached to the aircraft body frame in order to avoid some of the sources of error introduced by the gimbal mounts. The camera shutters and lidar are planned to be hardware-synchronized with the INS-GPS to substantially reduce time-offset uncertainty. The cameras would have global shutters and prime lenses.

While the primary objective of the flight segments so far has been to support the evaluation of SLAM [8,9] and COPOSIT [7] algorithms by closely associating the video frames with the ground-truth position and attitude, the team hopes to augment the datasets with additional annotations. In addition to precision location applications, computer vision is expected to play a key role in hazard avoidance in autonomous aviation. Future annotations could include airborne hazards such as birds, sUASs, and other aircraft or ground hazards such as towers, power lines, and people or objects within the landing area. The team is investigating sources of annotation data, such as geospatial databases, air traffic tracks, and onboard Remote ID logging for sUAS tracks [11].

Acknowledgements

The team thanks the groups and individuals who helped collect and assemble these datasets. The NASA Kennedy Space Center (KSC) (Kennedy Space Center, Florida) Flight Operations team, including Andre Karpowich, John Graves, and Shannon Gregory, supported the helicopter data collection. The NASA Armstrong Flight Research Center (AFRC) (Edwards, California) Dale Reed Subscale Flight Research Laboratory provided small unmanned aerial system (sUAS) flight support. Videographers Steve Parcel, Mike Agnew, and Jacob Shaw lent their talents on the sUAS camera operation. Chester Dolph and Thomas Lombaertz provided their experience and guidance. Interns Kelden Ben-Ora, Valerie Moore, and QiTao Weng contributed to the data processing tools.

References

- [1] Geiger, A. Lenz, P., and Urtasun, R., "Are we ready for autonomous driving? The KITTI Vision Benchmark Suite," in 2012 IEEE Conference on Computer Vision and Pattern Recognition, 2012, pp. 3354-3361.
- [2] Sun, P., et al. "Scalability in Perception for Autonomous Driving: Waymo Open Dataset," in *2020 IEEE/CVF Conference on Computer Vision and Pattern Recognition (CVPR)*, pp. 2443–2451, 2020.
doi: 10.1109/CVPR42600.2020.00252.
- [3] Nguyen, T.-M., Yuan, S., Cao, M., Nguyen, T., and Xie, L., "VIRAL SLAM: Tightly Coupled Camera-IMU-UWB-Lidar SLAM," in *The International Journal of Robotics Research*, 2022;41(3):270-280.
doi:10.1177/02783649211052312
- [4] Burri M., et al. "The EuRoC MAV datasets," in *The International Journal of Robotics Research*, January 2016.
doi:10.1177/0278364915620033
- [5] Campos, C., Elvira, R., Rodriguez, J. J. G. Montiel, J. J. M., and Tardós, J. D., "ORB-SLAM3: An Accurate Open-Source Library for Visual, Visual-Inertial, and Multimap SLAM," in *IEEE Transactions on Robotics*, Vol. 37, No. 6, December 2021, pp. 1874-1890.
doi: 10.1109/TRO.2021.3075644
- [6] Ferrera, M., Eudes, A., Moras, J., Sanfourche, M., and Le Besnerais, G., "OV2SLAM: A Fully Online and Versatile Visual SLAM for Real-Time Applications," in *IEEE Robotics and Automation Letters*, Vol. 6, No. 2, 2021, pp. 1399–1406.
URL:<https://doi.org/10.1109/LRA.2021.3058069>

- [7] Kawamura, E., Dolph, C., Kannan, K., Lombaerts, T., and Ippolito, C., “Simulated Vision-based Approach and Landing System for Advanced Air Mobility” AIAA Paper 2023-2195, January 2023.
doi: 10.2514/6.2023-2195
- [8] Kawamura, E., Dolph, C., Kannan, K., Brown, N., Lombaerts, T., and Ippolito, C., “VSLAM and Vision-based Approach and Landing for Advanced Air Mobility,” AIAA Paper 2023-2196, January 2023.
doi: 10.2514/6.2023-2196
- [9] Kannan, K., Chakrabarty, A., Baculi, J., Kawamura, E., Holforty, W., and Ippolito, C., “Comparison of Visual and LiDAR SLAM Algorithms using NASA Flight Test Data,” AIAA 2023-2679.c1, March 2023.
doi: 10.2514/6.2023-2679.c1
- [10] Zahn, D., et al., “UAM Instrument Flight Procedure Design and Evaluation in the Joby Flight Simulator,” NASA working paper AAM-NC-115-001, 2023. URL: <https://ntrs.nasa.gov/citations/20230003478>.
- [11] ASTM International, “Standard Specification for Remote ID and Tracking,” ASTM F3411-22a.
doi: 10.1520/F3411-22A